J. Astrophys. Astr. (2001) **22,** 309–319

A Map for a Group of Resonant Cases in a Quartic Galactic Hamiltonian

N. D. Caranicolas *Department of Physics, Section of Astrophysics, Astronomy and Mechanics, University of Thessaloniki, 540 06 Thessaloniki, Greece*
e-mail: caranic@helios.astro.auth.

Received 2000 October 11; accepted 2001 November 29

Abstract. We present a map for the study of resonant motion in a potential made up of two harmonic oscillators with quartic perturbing terms. This potential can be considered to describe motion in the central parts of non-rotating elliptical galaxies. The map is based on the averaged Hamiltonian. Adding on a semi-empirical basis suitable terms in the unperturbed averaged Hamiltonian, corresponding to the 1:1 resonant case, we are able to construct a map describing motion in several resonant cases. The map is used in order to find the $x - p_x$ Poincare phase plane for each resonance. Comparing the results of the map, with those obtained by numerical integration of the equation of motion, we observe, that the map describes satisfactorily the broad features of orbits in all studied cases for regular motion. There are cases where the map describes satisfactorily the properties of the chaotic orbits as well.

Key words. Galaxies: elliptical-orbits-regular and chaotic motion—maps: averaged Hamiltonian—stability.

1. Introduction

Resonant orbits are very important for systems of 2 degrees of freedom. Stable resonant tori give birth to families of regular orbits with similar shape to that of the parent resonant periodic orbit. On the other hand, unstable resonant tori are connected with a breakdown of regularity and with chaos.

One of the modern and quick methods to study the properties of orbits in a dynamical system is to use a map in order to construct the Poincare phase plane of a given Hamiltonian system. This technique was successfully used both in celestial mechanics and galactic dynamics (see Caranicolas 1990, 1994; Hadjidemetriou 1991, 1993; Sidlikovsky 1992; Hadjidemetriou & Lemaitre 1997; Caranicolas & Karanis 1999).

In this article we shall use the potential

$$V = \frac{1}{2}(\omega_1^2 x^2 + \omega_1^2 y^2) - \varepsilon\left[\beta(x^4 + y^4) + 2\alpha x^2 y^2\right], \tag{1}$$

where ω_1, ω_2 are the unperturbed frequencies of oscillation along the x and y axis respectively, α and β are positive parameters while $\varepsilon > 0$ is the perturbation strength.

This potential can be considered to describe the motion in the central parts of non rotating elliptical galaxies. We are particularly interested in resonant motion and for the study of the properties of resonant orbits we shall use a map. We aim to construct a map describing several resonant cases. The details for the construction of the map are given in section 2. Section 3 contains some applications while a discussion and the conclusions of this work are presented in section 4.

2. A map for a group of resonant cases

The Hamiltonian to the potential (1) is

$$H = \frac{1}{2}(p_x^2 + p_y^2) + V = h, \tag{2}$$

where p_x, p_y are the momenta per unit mass conjugate to x and y while h is the numerical value of H. In order to obtain the averaged Hamiltonian we follow the steps described in Caranicolas (1990). The averaged Hamiltonian in the resonant case $\omega_2 : \omega_1 = 1 : 1$ reads

$$\varepsilon\beta\left[\frac{3J^2}{2\omega_1^2} + \frac{3(\Lambda - \omega_1 J)^2}{2\omega_2^4}\right] + \frac{2\varepsilon\alpha J(\Lambda - \omega_1 J)}{\omega_1\omega_2^2}\left[1 + \cos 2\left(\theta - \frac{\pi}{2}\right)\right], \tag{3}$$

where we have set $\Lambda = h$. In order to study general resonance cases, say $\omega_2 : \omega_1 = r : s$, where r, s are integers, we must modify the Hamiltonian (3). A reasonable choice is to replace the term $\cos\,(2\theta - \pi)$ which characterizes the 1:1 resonance with the term $\cos\,(2r\theta - s\pi)$. In this way we obtain generally the Hamiltonian

$$\varepsilon\beta\left[\frac{3J^2}{2\omega_1^2} + \frac{3(\Lambda - \omega_1 J)^2}{2\omega_2^4}\right] + \frac{2\varepsilon\alpha J(\Lambda - \omega_1 J)}{\omega_1\omega_2^2}\left[1 + \cos 2\left(r\theta - s\frac{\pi}{2}\right)\right], \tag{4}$$

which gives (see for details Caranicolas 1990) generally the map

$$\begin{aligned} J_{n+1} &= J_n + f(J_{n+1}, \theta_n) \\ \theta_{n+1} &= \theta_n + S(J_{n+1}) + g(J_{n+1}, \theta_n), \end{aligned} \tag{5}$$

where

$$\begin{aligned} f(J,\theta) &= \pm\frac{2\varepsilon\alpha r J(\Lambda - \omega_1 J)\sin 2r\theta}{\omega_1\omega_2^2}, \\ S(J) &= \frac{3\varepsilon\beta J}{\omega_1^2} - \frac{3\varepsilon\beta\omega_1(\Lambda - \omega_1 J)}{\omega_1^4} - \frac{2\varepsilon\alpha J}{\omega_2^2} + \frac{2\varepsilon\alpha(\Lambda - \omega_1 J)}{\omega_1\omega_2^2}, \\ g(J,\theta) &= \pm\frac{\varepsilon\alpha(\Lambda - 2\omega_1 J)\cos 2r\theta}{\omega_1\omega_2^2}. \end{aligned} \tag{6}$$

We use the plus sign when $s = 2k$ and the minus sign when $s = 2k+1, k = 0, 1, 2\ldots$ and return to the original x, p_x variables through $x = (2J/\omega_1)^{1/2}\cos\varphi,\ p_x = -(2J\omega_1)^{1/2}\sin\varphi$.

The fixed points of (5) are at

$$
\begin{aligned}
&\text{(i)} \quad J = \frac{\omega_1(\beta\omega_1^2 - \alpha\omega_2^2)\Lambda}{\beta\omega_1^4 - 2\alpha\omega_1^2\omega_2^2 + \beta\omega_1^4}\ , \qquad \theta = 0, \pi,\\
&\text{(ii)} \quad J = \frac{\omega_1(3\beta\omega_1^2 - \alpha\omega_2^2)\Lambda}{3\beta\omega_1^4 - 2\alpha\omega_1^2\omega_2^2 + 3\beta\omega_1^4}\ , \qquad \theta = \pm\frac{\pi}{2}, \qquad (7)\\
&\text{(iii)} \quad J = 0, \qquad \text{any } \theta.
\end{aligned}
$$

Here we must make clear that we have the above positions of the resonant fixed points (i) and (ii) when $s = 2k$ while, for $s = 2k+1$, the fixed points (i) and (ii) interchange their θ positions.

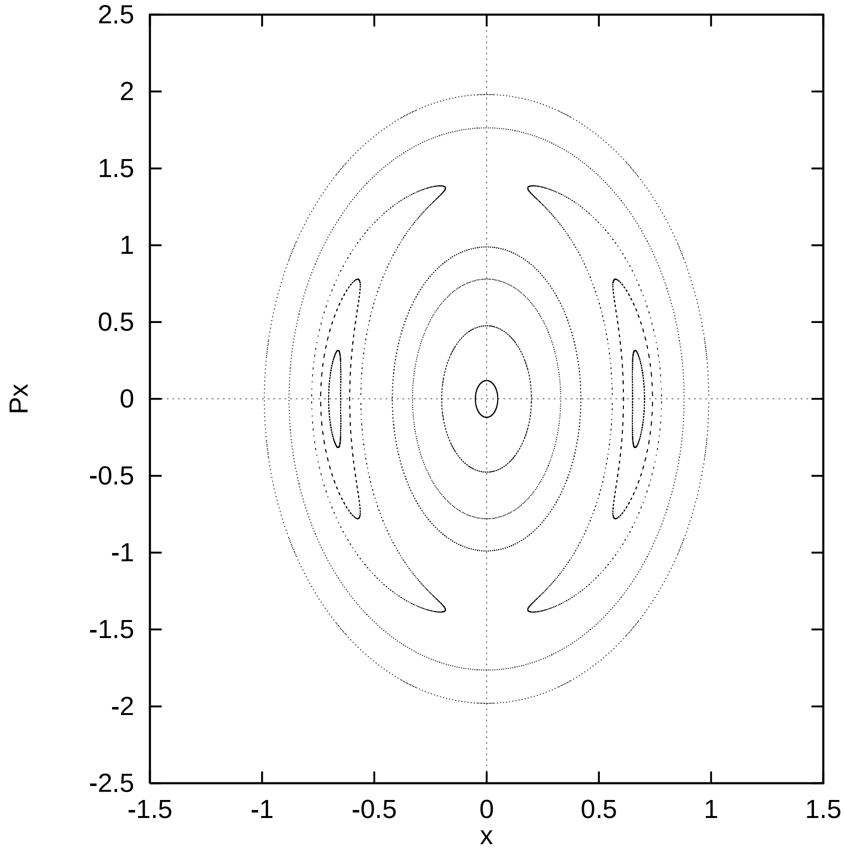

Figure 1. The $x - p_x$ phase plane, in the case of the 2:1 resonance, derived by numerical integration. The values of the parameters are $\varepsilon = 0.1,\ h = 2,\ \alpha = 1.2,\ \beta = 0.01$.

3. Applications

The general map (5) gives very good results in the 1:1 resonance case. This case has been studied in detail by Caranicolas & Vozikis (1999). In the following we shall use the map (5) in order to study the properties of orbits in two additional resonance cases: the 2:1 and the 3:1 resonant case.

3.1 *The 2:1 resonance*

In order to make things simple we use the values $\omega_1 = 2, \omega_2 = 1$. In this case the positions of the resonant periodic points are given by

$$\text{(i)} \quad J = \frac{2(\alpha - 4\beta)\Lambda}{8\alpha - 17\beta}, \qquad \theta = 0, \pi,$$

$$\text{(ii)} \quad J = \frac{2(\alpha - 12\beta)\Lambda}{8\alpha - 51\beta}, \qquad \theta = \pm\frac{\pi}{2}. \tag{8}$$

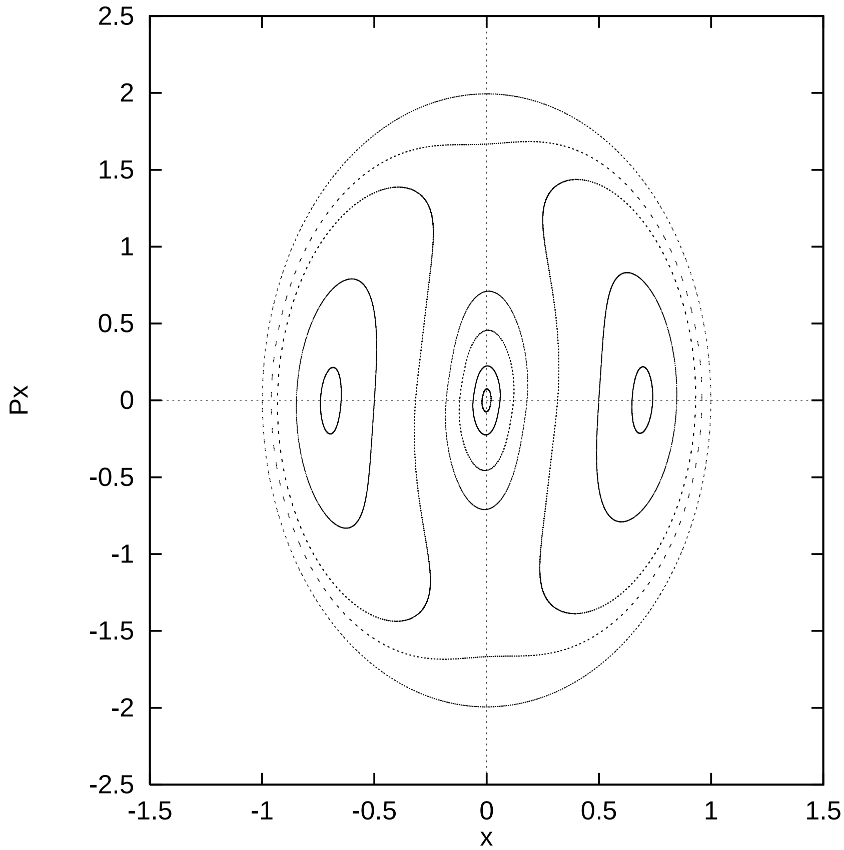

Figure 2. The $x - p_x$ phase plane, in the case of the 2:1 resonance, derived by the map. The values of the parameters are as in Fig. 1.

It is evident that the existence, position and stability of the resonant periodic orbits depends on the particular values of the parameters α and β. An elementary analysis shows that both resonant periodic orbits (i) and (ii) are present when

$$\alpha > 12\beta \tag{9}$$

while only the resonant periodic points (i) are present when

$$\frac{51\beta}{8} < \alpha < 4\beta. \tag{10}$$

The indices of stability (see Caranicolas 1990) for the resonant periodic orbits (i) and (ii) are

$$\begin{aligned} \delta_1 &= \left| 2 + \frac{3\alpha}{8\alpha - 17\beta} \left[9\alpha\beta - 4(\alpha - \beta)^2 \right] \varepsilon^2 \Lambda^2 \right|, \\ \delta_2 &= \left| 2 + \frac{\alpha}{8\alpha - 51\beta} \left[4(\alpha^2 + 9\beta^2) - 51\alpha\beta \right] \varepsilon^2 \Lambda^2 \right| \end{aligned} \tag{11}$$

respectively. When $\delta < 2$ the orbit is stable, otherwise it is unstable.

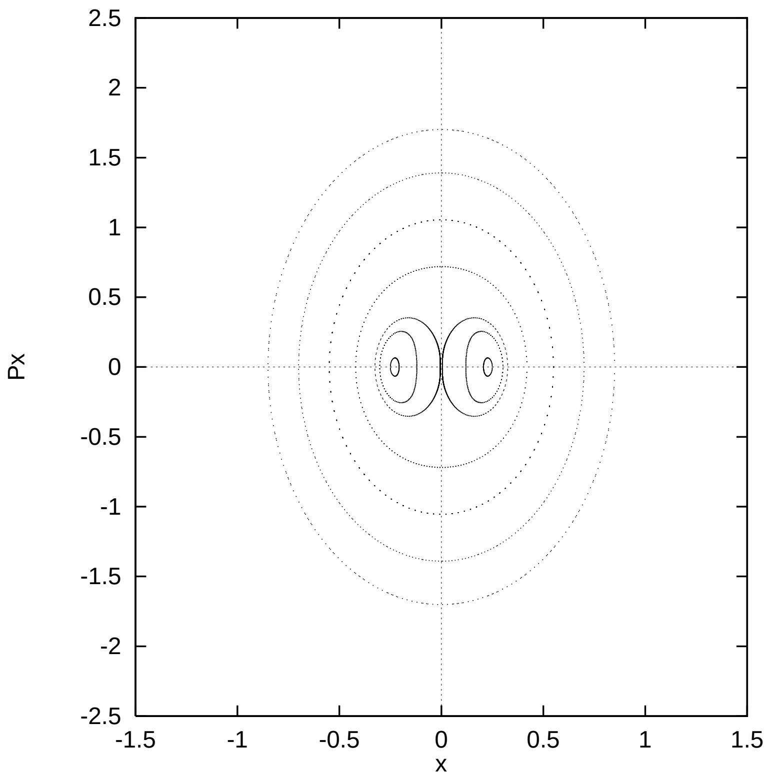

Figure 3. Same as Fig. 1 when $\beta = 0.1$.

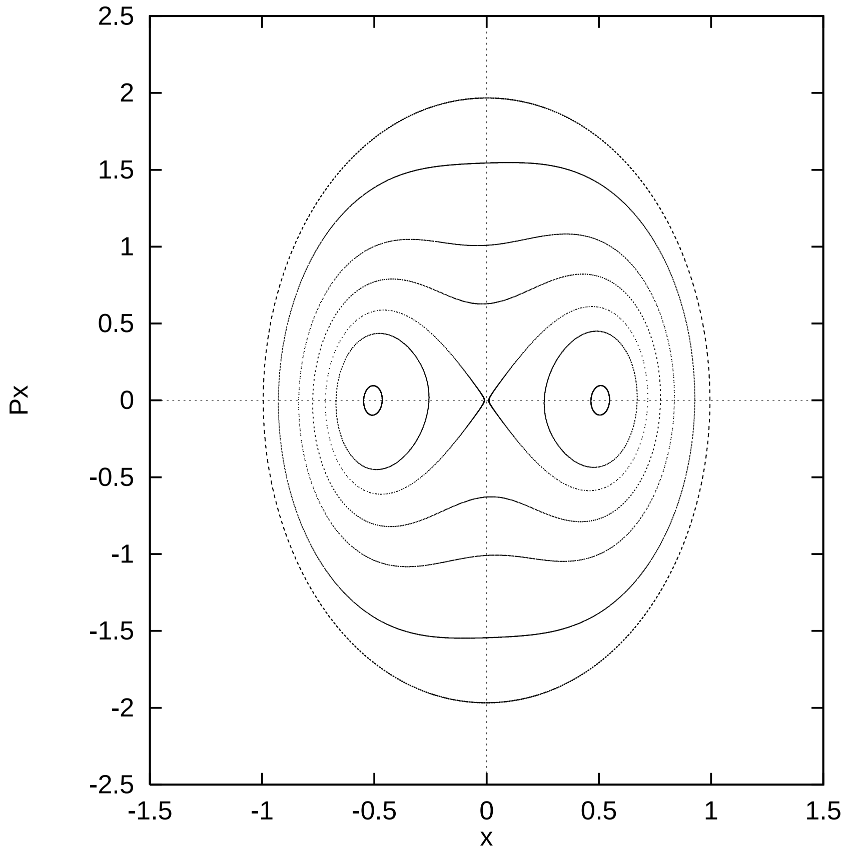

Figure 4. Same as Fig. 2 when $\beta = 0.1$.

Figures 1 and 2 show the x-p_x phase plane, when $\alpha = 1.2,\ \beta = 0.01,\ h = 2,\ \varepsilon = 0.1$, found by numerical integration and the map respectively. As one can see the basic characteristic, that is position of periodic points and stability, are satisfactorily described by the map. It is evident that we are in the case (9) where both fixed points (i) and (ii) are present. As, in this case, β is at least two orders of magnitude smaller than α, relations (11) give $\delta_1 < 2,\ \delta_2 > 2$, which means that fixed points (i) are stable while fixed points (ii) are unstable. Figs. 3 and 4 are similar to 1 and 2 when $\beta = 0.1$. One observes that the resonant periodic points (ii) are not present now, because for this value of β relation (10) is valid. We see that the position of the periodic orbits is not the same in the two patterns. Nevertheless the general topology and the stability features of the phase plane derived by the map is similar to that given by the real system.

3.2 *The 3:1 resonance*

In what follows we shall study the 3:1 resonance. Here we use the values $\omega_1 = 3,\ \omega_2 = 1$. The position of the resonant periodic points, which become again functions of the parameters α and β are at

$$
\begin{aligned}
&\text{(i)} \quad J = \frac{(\alpha - 27\beta)\Lambda}{2(8\alpha - 41\beta)}, \qquad \theta = 0, \pi, \\
&\text{(ii)} \quad J = \frac{3(\alpha - 9\beta)\Lambda}{2(9\alpha - 41\beta)}, \qquad \theta = \pm\frac{\pi}{2}.
\end{aligned} \tag{12}
$$

Both resonant periodic orbits (i) and (ii) are present when

$$\alpha > 27\beta \tag{13}$$

while only the resonant periodic points (i) are present when

$$9\beta < \alpha < 27\beta. \tag{14}$$

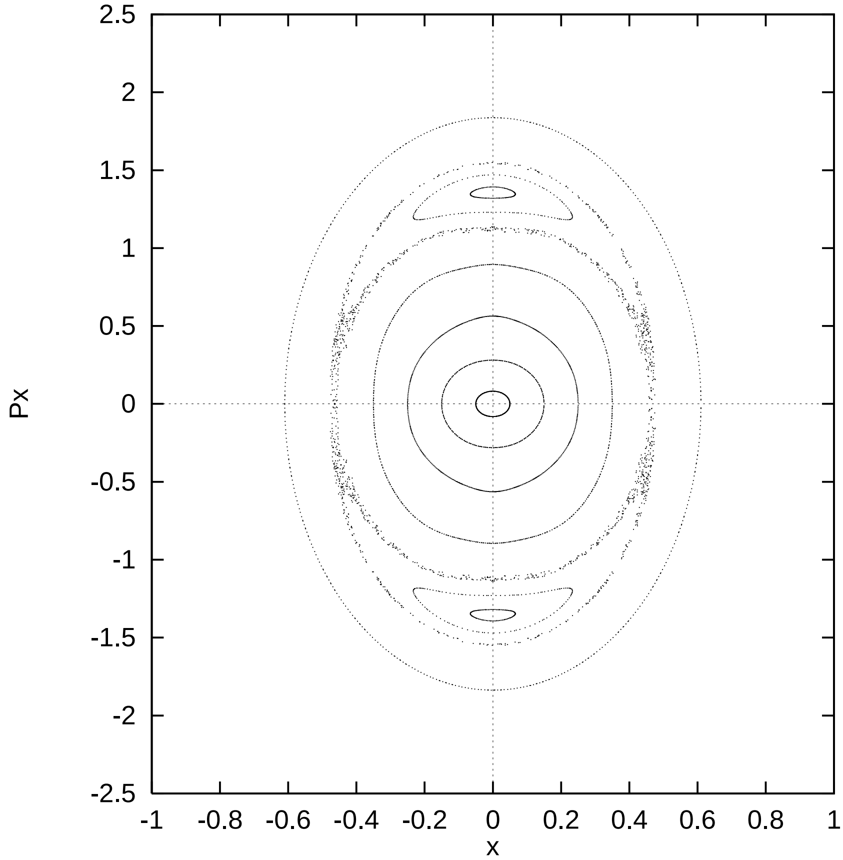

Figure 5. The $x - p_x$ phase plane, in the case of the 3:1 resonance, derived by numerical integration. The values of the parameters are $\varepsilon = 0.4,\ h = 2,\ \alpha = 1.2,\ \beta = 0.01$.

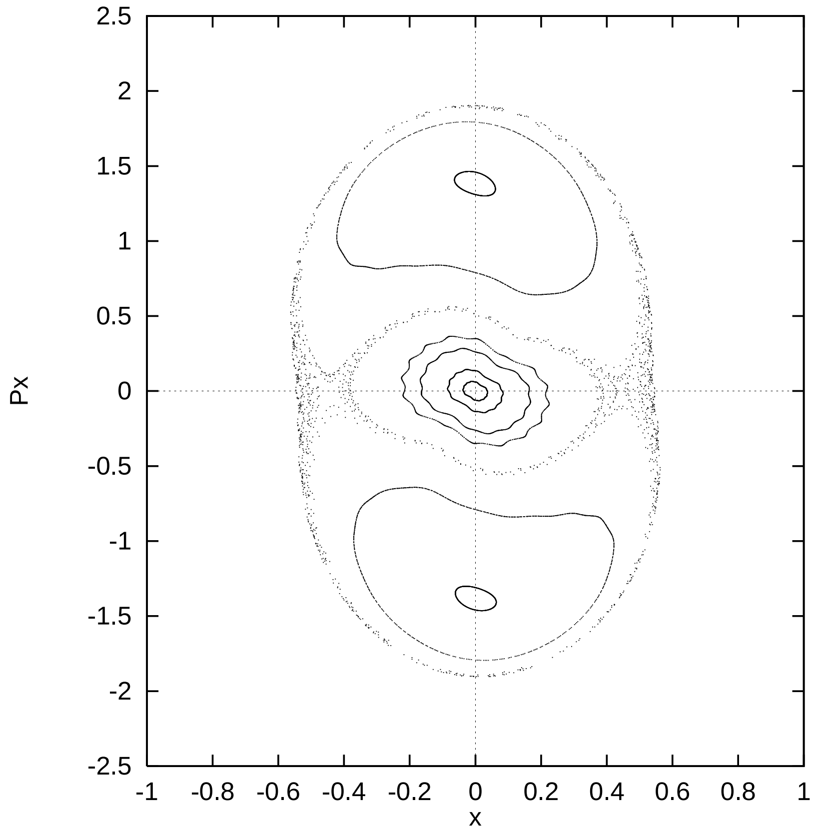

Figure 6. The $x - p_x$ phase plane, in the case of the 3:1 resonance, derived by the map. The values of the parameters are as in Fig. 5.

In this resonant case the indices of stability, for the resonant periodic orbits (i) and (ii), become

$$\delta_1 = \left| 2 + \frac{2\alpha}{9(3\alpha - 41\beta)} \left[3(\alpha - \beta)^2 - 4\beta(19\alpha - 6\beta) \right] \varepsilon^2 \Lambda^2 \right|,$$

$$\delta_2 = \left| 2 + \frac{2\alpha}{3(9\alpha - 41\beta)} \left[64\alpha\beta - 9(\alpha - \beta)^2 \right] \varepsilon^2 \Lambda^2 \right|, \tag{15}$$

respectively.

Figures 5 and 6 show the $x - p_x$ phase plane found by numerical integration and the map respectively. The values of the parameters are $\alpha = 1.2$, $\beta = 0.01$, $h = 2$, $\varepsilon = 0.4$. Here one observes that part of the phase plane appears chaotic. This chaotic behavior is also described by the map. Finally Figs. 7 and 8 are similar to Figs. 5 and 6 but when $\beta = 0.1$, $\varepsilon = 0.25$. Here the motion is regular, the central point is unstable while the resonant points (i) are not present. As one can see the position of the resonant points is different in the two patterns. On the other hand, we observe that the structure of and the stability characteristics are the same for the two phase planes.

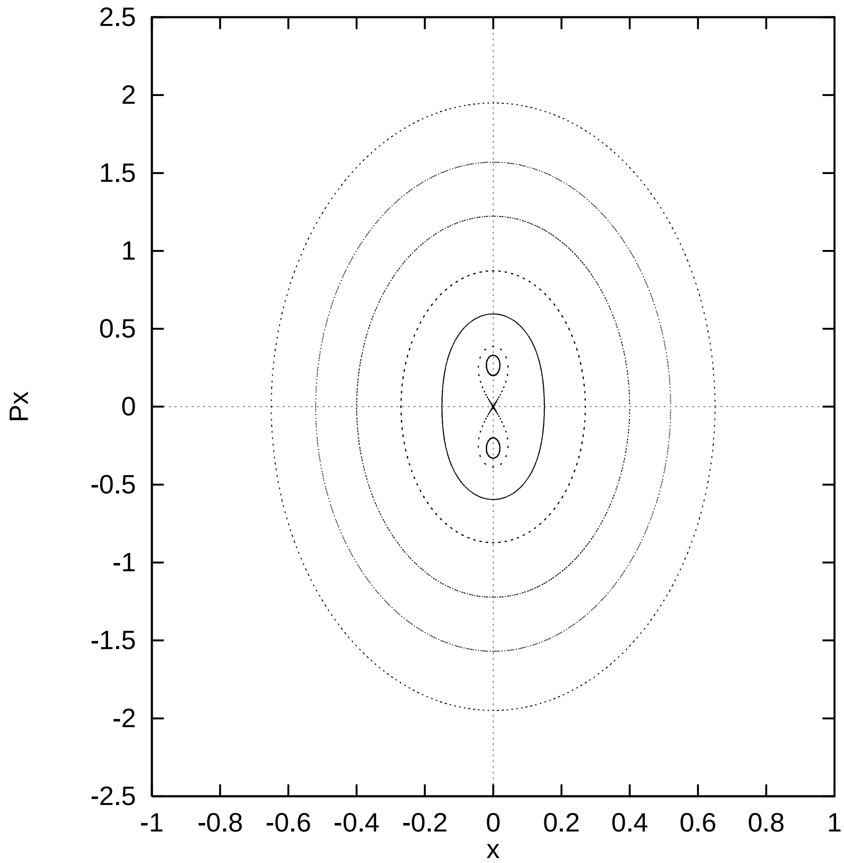

Figure 7. Same as Fig. 5 when $\varepsilon = 0.25$, $\beta = 0.1$.

4. Discussion

In this paper we have tried to present a map describing three different resonant cases. Of course it is not easy to find a map describing all resonance cases. In an earlier paper (Caranicolas & Vozikis 1999) we have constructed a map, describing the Hamiltonian system (2) in the 1:1 resonant case. That map gave results that are in very good agreement with those found by numerical integration. The construction of the map, in the 1:1 resonant case was easy because, for the particular resonance, the Hamiltonian to the potential (1) had suitable terms that favored the above resonant case. On the other hand numerical evidence suggests that the quartic Hamiltonian (2) gives interesting results for other resonant cases as well.

On this basis we decided to construct a map that will be adequate to cover several resonant cases instead of one single resonance. One additional reason for this decision was that the map gives analytic expressions for the position and stability of the resonant periodic orbits of the system. Furthermore, the idea to have a tool, that is the map, that describes a group of resonances seems interesting and attractive.

What we have presented here is a semi-analytical method. In fact we have replaced in the averaged Hamiltonian (3) the term depending on the angle θ by a general term,

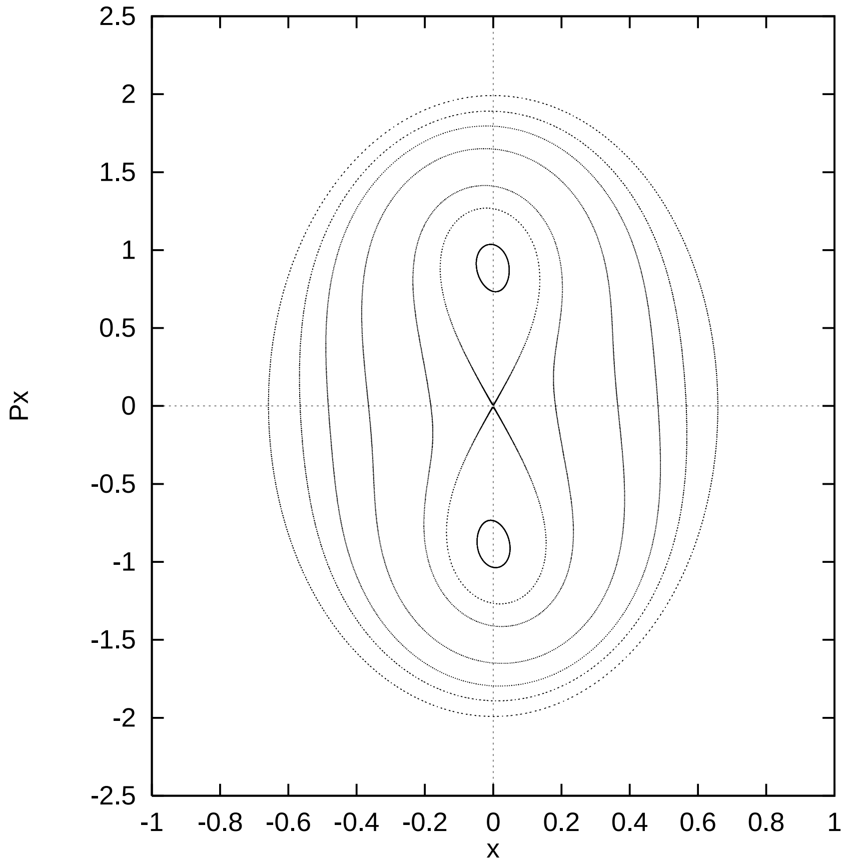

Figure 8. Same as Fig. 6 when $\varepsilon = 0.25$, $\beta = 0.1$.

containing the integers r and s, in such a way as to cover some additional resonant cases. This was made in a complete empirical basis and our choice was justified by the satisfactory results. Here we must emphasize that semi-analytical or semi-numerical methods are of importance and have been frequently used both in galactic dynamics and celestial mechanics during the last years (see Henrard & Lemaitre 1986, 1987; Henrard 1990; Henrard & Sato 1990; Caranicolas & Innanen 1992; Caranicolas 1993).

The results of this work suggest that maps can give fast, interesting and analytical information for systems made up of harmonic oscillators not only for a particular resonance but for several resonant cases. We believe that it is not too difficult to construct a map, for any resonant case, in systems made up of perturbed harmonic oscillators. What we have to do is to replace or to add suitable terms in an averaged Hamiltonian coming from the real system. This will make maps more useful and stronger tools for the study of the nice properties of harmonic oscillators. The reader can find interesting information on the construction and use of maps in Lichtenberg & Lieberman (1983) and Hadjidemeriou (1991). Another interesting and powerful tool, for systems made up of harmonic oscillators, is the extension of the lissajous transformation for the study of the phase space of the above systems in any resonant case (see Elipe & Deprit 1999; Elipe 2000).

Acknowledgement

The author would like to thank an anonymous referee for useful comments.

References

Caranicolas, N. D. 1990, *Cel. Mech.* **47**, 87.
Caranicolas, N. D. 1993, *Astr. Astrophys.* **267**, 388.
Caranicolas, N. D. 1994, *Astr. Astrophys.* **287**, 752.
Caranicolas, N. D., Karanis, G. I. 1999, *Astr. Astrophys.* **342**, 389.
Caranicolas, N. D. Vozikis, Ch. 1999, *Astr. Astrophys.* **349**, 70.
Caranicolas, N. D. 2000, *New Astron.* **5**, 397.
Caranicolas, N. D., Innanen, K. A. 1992, *Astron. J.* **103**, 1308.
Elipe, A., Deprit, A. 1999 *Mech. Res. Com.* **26**, 635.
Elipe, A. 2000 *Phys. Rev. E.* **61**, 6477.
Hadjidemetriou, J. D. 1991 *Mapping Models for Hamiltonian Systems with application to Resonant Asteroid Motion*, in *Predictability, Stability and Chaos in N-Body Dynamical Systems*, A E Roy (ed.) 157, (Kluwer Publ.)
Hadjidemetriou, J. D. 1993, *Cel. Mech.* **56**, 563.
Hadjidemetriou, J. D., Lemaitre, A. 1997, *The dynamical behaviour of our planetary system*, p.277, (Kluwer Academic Publishers)
Henrard, J. 1990, *Cel. Mech.* **49**, 43.
Henrard, J., Lemaitre, A. 1986, *Cel. Mech.* **39**, 213.
Henrard, J., Lemaitre, A. 1987, *Icarus* **69**, 266.
Henrard, J., Sato, M. 1990, *Cel. Mech.* **47**, 391.
Lichtenberg, A. J., Lieberman, M. A. 1983, *Regular and stochastic motion*, (Berlin Heidelberg; New York: Springer)
Sidlichovsky, M. 1992, *Astron. J.* **87**, 577.